The Dynamics of Coastally Trapped Mesoscale Ridges in the Lower Atmosphere

C. J. C. REASON AND D. G. STEYN

Atmospheric Science Programme, Departments of Geography and Oceanography and Institute of Applied Mathematics, The University of British Columbia, Vancouver, British Columbia, Canada

(Manuscript received 31 July 1991, in final form 13 November 1991)

ABSTRACT

The dynamics of coastally trapped ridges that propagate in the marine layers of western North America and southeastern Australia is examined. A nonlinear semigeostrophic theory shows that the coastal ridges develop initially as an alongshore intrusion of denser marine air that is driven by the synoptic-scale pressure gradient. Nonlinear Kelvin waves evolve with the intruding flow on a slower time scale governed by the dynamic parameters. If dispersive effects balance the nonlinearities, then these waves evolve into solitary form. Otherwise, the nonlinear waves steepen so that the leading edge of the ridge eventually propagates as a shock.

The theory is applied to two ridging events in California and one in southeastern Australia. In each case, good agreement is found between theory and observations of the evolution times and propagation speeds of the coastal ridges. The theory also explains the observed behavior of the events at prominent convex bends and gaps in the coastal topography.

1. Introduction

The phenomenon of intrusion of fluid along the side boundary of a fluid of different density has been extensively studied in rotating tank experiments (Stern et al. 1982; Griffiths and Hopfinger 1983; Maxworthy 1983; Kubokawa and Hanawa 1984, hereafter referred to as KH; Simpson 1987). These studies have shown that the intrusion occurs as some form of gravity current (i.e., a mainly horizontal flow driven by density differences) whose width is limited by rotational effects to the order of the Rossby radius and that associated with the main current are various propagating waves. Such coastal intrusions of buoyant fluid are often observed in the oceans—examples are the Kyucho coastal currents in Japan (Yamagata 1980; KH), the East Greenland Current (Wadhams et al. 1979), and the Leeuwin Current off Western Australia (Griffiths 1986).

In the atmosphere, it is conceivable that under suitably stratified and synoptically forced conditions, barrierlike coastal mountain ranges may act as a side boundary and so allow intrusions of dense air alongshore. The most obvious example would be if a marine subsidence inversion exists at a height below the mountain crests. Then a low-level intrusion would be confined vertically by this inversion and laterally by Coriolis trapping against the coastal mountains. This situation is often found during summer along the California (Dorman 1985, 1987; Mass and Albright 1987) and southeastern Australia coasts (Holland and Leslie 1986). All these authors observed a mesoscale low-level ridge of dense air that intruded along the coastal mountain ranges over a time span of a few days and that was confined to a coastal zone approximately a Rossby radius in width. The dynamics of these ridges have been variously interpreted as a Kelvin wave (Dorman 1985), a coastal gravity current (Dorman 1987), a flow with both a coastal gravity current and a Kelvin wave component (Holland and Leslie 1986), and an ageostrophic downgradient flow controlled by synoptic-scale pressure changes (Mass and Albright 1987).

One reason for the differences in interpretation is the mesoscale nature of the ridges. Even an intensive field program (CODE 82) along the central California coast had insufficient spatial and temporal resolution to reveal much more than the coarsest features of the ridges (Dorman 1985, 1987). This leads to obvious difficulties in making unambiguous interpretations. Another reason for differences of interpretation is the lack of a suitable theoretical framework. The Dorman (1985, 1987), Holland and Leslie (1986), and Mass and Albright (1987) studies were largely descriptive and did not explicitly consider nonlinear effects. To improve this state of affairs, the following approach is adopted. First, a more general theory than hitherto available is developed for the coastal ridges. Then the available data are reanalyzed in terms of that theory and, where appropriate, the analogs between rotating-tank experiments and oceanic and atmospheric dis-

Corresponding author address: Dr. C. J. C. Reason, School of Mathematical and Physical Sciences, Murdoch University, Murdoch (Perth), WA 6150, Australia.

turbances are emphasized in order to arrive at a better understanding of the behavior of the coastal ridges. Specifically, it is shown that the dynamics of the ridges may be described as a synoptically forced intrusion that is coastally trapped and may, under certain conditions, have a propagating nonlinear Kelvin wave associated with it. By including both synoptic pressure gradients and nonlinear effects and by showing that the resulting ageostrophic alongshore flow of the intrusion may evolve into either a solitary Kelvin or a shock wave component, the analysis (see sections 2 and 3c) generalizes the various specific interpretations of the aforementioned authors. To accomplish this generality, the model includes both nonlinear and dispersive effects through a perturbation expansion of the governing shallow-water equations for a rotating, stratified fluid and is based on the work of KH, who considered a similar problem in coastal ocean dynamics.

2. Nonlinear semigeostrophic theory of coastally trapped disturbances

Since the intrinsic period of the coastally trapped disturbances is much greater than the buoyancy period and since typical horizontal length scales (a Rossby radius or greater) of these disturbances are much longer than the scale height (about 8–10 km) of the atmosphere, the dynamics will be well described by the hydrostatic approximation (e.g., Gill 1982). Thus, the shallow-water equations of motion are appropriate. Also, the essential vertical structure of the coastal atmosphere (e.g., Dorman 1985, 1987; Holland and Leslie 1986; Mass and Albright 1987; Reason 1989) has been observed to consist of an inversion separating a roughly constant density cool marine layer from a deep upper layer with weak winds; thus, a reduced gravity model of the stratification is a useful first approximation:

$$\frac{\partial u}{\partial t} + u\frac{\partial u}{\partial x} + v\frac{\partial u}{\partial y} - fv = -g'\frac{\partial h}{\partial x} + F_1 \qquad (2.1)$$

$$\frac{\partial v}{\partial t} + u\frac{\partial v}{\partial x} + v\frac{\partial v}{\partial y} + fu = -g'\frac{\partial h}{\partial y} + F_2 \qquad (2.2)$$

$$g' = g(\theta_2 - \theta_1)/\theta_2$$

$$\frac{\partial h}{\partial t} + \frac{\partial hu}{\partial x} + \frac{\partial hv}{\partial x} = 0. \qquad (2.3)$$

In (2.1)–(2.3), u and v are the across-shore and alongshore velocities, respectively, in the marine layer, h is the height of the inversion that separates the marine from the upper layer, f is the Coriolis parameter, g' is the reduced gravity of the two-layer atmosphere, θ_1 and θ_2 are the respective potential temperatures of the upper and lower (marine) layers, and F_1 and F_2 are forcing terms such as synoptic pressure gradients.

It is assumed that the coastal mountains may be represented by an infinitely long, vertical barrier, which is a good approximation if these mountains are sufficiently steep and if their radius of curvature is significantly greater than the Rossby radius or offshore scale of the motion (Gill 1977). Both the coastal mountains of western North America and southeastern Australia satisfy these constraints. It is also assumed that the inversion height is lower than the mountain crests, as is observed (Dorman 1985, 1987; Holland and Leslie 1986).

Most existing models of coastally trapped disturbances (e.g., Anh and Gill 1981; Bannon 1981; Dorman 1985; Griffiths 1986) make the simplification that the nonlinear advection terms are negligible. By making this simplification and by neglecting synoptic forcing and topographic variations, the equations are easily solvable analytically to yield either a free linear Kelvin wave or a coastal intrusion. In this simple linear case, it is solely the boundary conditions that determine which of these independent solutions is appropriate. For example, assuming that the alongshore velocity and inversion displacement vanish infinitely far from the coast leads to the standard coastal Kelvin wave solution (e.g., Gill 1982), whereas assuming the existence of a density front separating the disturbance flow from the ambient coastal atmosphere at a finite distance offshore and at which the inversion displacement is zero yields an alongshore intrusion. The intrusion solution is dependent on a known alongshore velocity at the coast (e.g., Griffiths 1986).

To show that the coastal intrusion and Kelvin wave solutions to (2.1)–(2.3) are related, a perturbation expansion of these equations is performed. A similar analysis has been presented by KH for a coastally trapped disturbance in the ocean. The model of these authors is extended here to consider dissipative effects due to gaps (e.g., valleys) in the coastal mountains and is modified by the use of a slightly different small parameter. It is also shown how forcing, in the form of an external synoptic pressure gradient, can be included. Observations (Dorman 1985, 1987; Holland and Leslie 1986; Mass and Albright 1987) show the coastal ridges to have time scales of a few days, across-shore length scales on the order of the internal Rossby radius R (100–300 km), much less than the observed alongshore length scale ($\geq$1000 km), and observed alongshore velocities on the order of the long-wave speed fR, which is much greater than the across-shore velocity (observed to be negligible). Hence, as in KH, time is scaled by the reciprocal of the Coriolis parameter multiplied by a parameter d, the alongshore displacement by R/d, the across-shore displacement by R, the alongshore velocity by fR, the across-shore velocity by fRd, and the inversion height by its climatologic value, H. Forcing, in the form of external synoptic pressure gradients ($\partial P/\partial x$, $\partial P/\partial y$), is similarly scaled (e.g., Gill 1977) so that (2.1)–(2.3) become

$$d^2\left[\frac{\partial u}{\partial t} + u\frac{\partial u}{\partial x} + v\frac{\partial u}{\partial y}\right] - v = -\frac{\partial h}{\partial x} - \frac{\partial P}{\partial x} \quad (2.4)$$

$$\frac{\partial v}{\partial t} + u\frac{\partial v}{\partial x} + v\frac{\partial v}{\partial y} + u = -\frac{\partial h}{\partial y} - \frac{\partial P}{\partial y} \quad (2.5)$$

$$\frac{\partial h}{\partial t} + \frac{\partial hu}{\partial x} + \frac{\partial hv}{\partial y} = 0, \quad (2.6)$$

where

$$d = \left[\frac{RH}{aL^*}\right]^{5/3}, \quad (2.7)$$

with L^* being an alongshore length scale and a being a typical amplitude of the disturbance. This definition differs from the semigeostrophic factor, R/L^*, used by KH and has been introduced so as to have a direct measure of nonlinearity (a/H) in the analysis.

In addition, the analysis requires the conservation of potential vorticity. Cross-differentiating (2.4) and (2.5), followed by subtraction and then substitution from (2.6), leads to an equation expressing this conservation. Assuming the initial potential vorticity (in dimensional units) to be f/H_0, where H_0 is the initial value of the inversion height and $k^2 = H_0/H$, leads to the form

$$\frac{\partial v}{\partial x} - d^2\frac{\partial u}{\partial y} + l = k^2 h. \quad (2.8)$$

Following KH, the solutions of (2.4)–(2.8) are then separated into semigeostrophic (subscripted s) and ageostrophic (subscripted a) parts;

$$u = u_s + d^2 u_a$$
$$v = v_s + d^2 v_a$$
$$h = h_s + d^2 h_a. \quad (2.9)$$

The semigeostrophic part will be an exact solution if the limit d^2 tends to 0.

Appropriate boundary conditions for the coastal atmosphere are that h, the inversion height, vanishes at a density front $x = -L(y, t)$, which separates the disturbance flow from the surrounding atmosphere (Fig. 1a). Note that in the limit of L becoming infinite, the boundary condition reduces to the standard Kelvin wave condition. In addition, it is assumed, as in KH, that the across-shore velocity vanishes at the coastal mountains and that the alongshore velocity at the density front $x = -L(y, t)$ is given by the convective derivative of this frontal position. Hence, the boundary conditions are

at the coast: $x = 0$; $u = 0$ and (2.10)

at the front: $x = -L(y, t)$; $u = DL/Dt$, $h = 0$. (2.11)

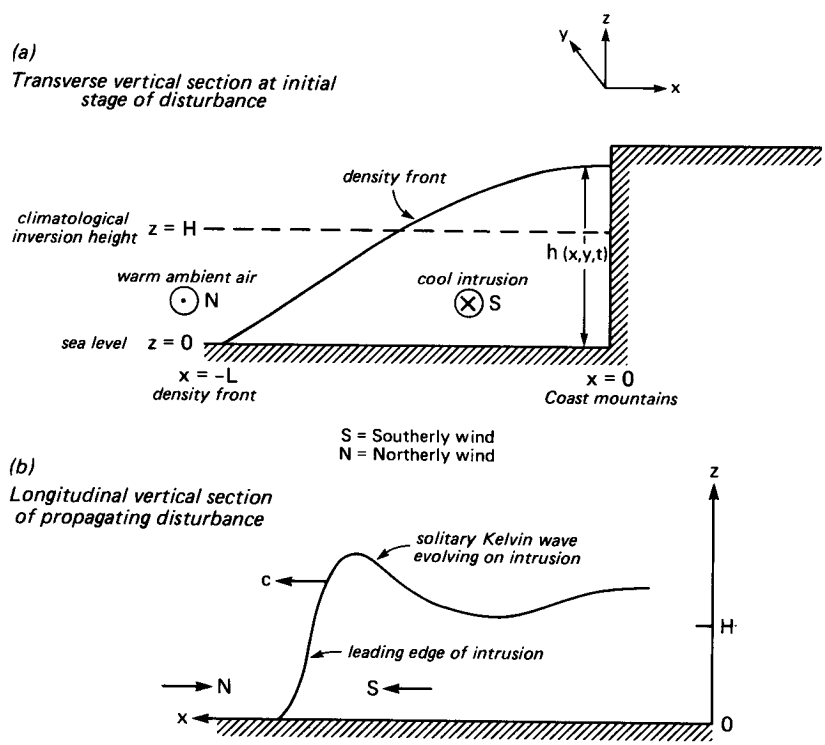

FIG. 1. Vertically exaggerated schematic showing (a) transverse and (b) longitudinal sections of inversion displacement during a coastally trapped ridging event.

Motivation for (2.11) (e.g., KH; Griffiths 1986) is that the density front separates the cooler, denser fluid of the intrusion from the warmer, less dense ambient atmosphere with no exchange between the two (Fig. 1a). Mixing processes are therefore ignored. Thus, the front is a material boundary and acts as a free streamline, so that fluid elements on this streamline remain there for all times. Unfortunately, the available offshore data are unable to show whether a density front like that observed in rotating-tank experiments and in the coastal ocean (e.g., Stern et al. 1982; Griffiths and Hopfinger 1983; KH; Griffiths 1986) actually occurs in the coastal atmosphere. However, satellite images presented by Dorman (1982, 1985) and Holland and Leslie (1986) show a sharp discontinuity in low-level cloud cover at about one Rossby radius offshore, which indicates the existence of such a density front during the ridging events. This follows because it is known from sounding data (Dorman 1982, 1985; Holland and Leslie 1986; Reason 1989) that there is cooler and denser air beneath the coastal inversion and that this inversion is raised by the forcing. As a result, the denser air reaches its condensation level to form cloud. The warmer and drier air offshore is not raised by the forcing so that no cloud forms there. Hence, the offshore discontinuity in low-level cloud indicates the boundary between the denser air of the intrusion and the warmer ambient air—this boundary is modeled as a density front.

Setting d^2 and, for convenience, the synoptic forcing $\partial P/\partial x$ and $\partial P/\partial y$ to zero then yields the semigeostrophic solution (as in KH) for the domain of interest $-L < x < 0$ (i.e., the coastal zone):

$$v_s = -k^{-1}\sinh[k(L+x)] + V(y,t)\cosh[k(L+x)] \quad (2.12)$$

$$h_s = k^{-2}\{1 - \cosh[k(L+x)] + kV(y,t)\sinh[k(L+x)]\}, \quad (2.13)$$

where $V(y,t)$ is the alongshore velocity at the density front. For $x < -L$, that is, seawards of the coastal zone of interest, the motion may be assumed to vanish. Upon substituting (2.12) and (2.13) back into (2.5) and evaluating at $x = 0$ and $-L$, the following nonlinear system is obtained:

$$\frac{\partial \mathbf{V}}{\partial t} + \mathbf{B}\frac{\partial \mathbf{V}}{\partial y} = 0, \quad (2.14a)$$

where $\mathbf{V}$ is a vector containing components (V, L) and $\mathbf{B}$ is a 2×2 matrix that is a function of $\mathbf{V}$. The components of matrix $\mathbf{B}$ are given in Eqs. (A1) to (A4) of KH. If synoptic forcing is included, then (2.14a) becomes

$$\frac{\partial \mathbf{V}}{\partial t} + \mathbf{C}\frac{\partial \mathbf{V}}{\partial y} = -\frac{\partial \mathbf{P}}{\partial y}, \quad (2.14b)$$

where $\mathbf{P}$ is a vector containing this forcing evaluated at $x = 0, -L$ and where the matrix $\mathbf{C}$ will have slightly different components to those of $\mathbf{B}$, that will depend on the modification to (2.12) and (2.13) by the forcing. This modification will not alter the evolution of the solitary wave derived below because this wave is an asymptotic solution and is therefore essentially independent of precisely how it is formed. In other words, the solitary wave develops on an asymptotically long time scale (see below) compared to that of the external forcing that generates the initial disturbance—this forcing will therefore influence the shape of the initial flow [(2.12) and (2.13)] but will become insignificant [e.g., synoptic maps in Mass and Albright (1987; Figs. 23–25) show the forcing removed from the coastal region within about one day] on the long time scale on which the solitary wave evolves. Hence, the only effect of nonzero external forcing is to modify the exact displacement and velocity profiles of the initial intrusion.

Using standard techniques (see, for example, Whitham 1974), (2.14a) is multiplied by the left eigenvector $\mathbf{l}$ of the matrix $\mathbf{B}$ so that the characteristic form (2.15) results:

$$\mathbf{l}\frac{d\mathbf{V}}{dt} = 0 \quad \text{on} \quad \frac{dy}{dt} = c \quad \text{with} \quad \mathbf{lB} = \mathbf{l}c. \quad (2.15)$$

If external forcing is included, then (2.15) is replaced by

$$\mathbf{l}^*\frac{d\mathbf{V}}{dt} + \mathbf{P}' = 0 \quad \text{on} \quad \frac{dy}{dt} = c, \quad (2.16)$$

where $\mathbf{l}^*$ is the left eigenvector of the matrix $\mathbf{C}$, $\mathbf{l}^*\mathbf{C} = \mathbf{l}^*c$, and $\mathbf{P}'$ is the pressure gradient term.

Equations (2.15) and (2.16) are hyperbolic systems that represent two independent waves that evolve on the mean intrusion and that have phase speeds given by the two characteristic velocities or eigenvalues c of the 2×2 matrices $\mathbf{B}$ or $\mathbf{C}$ (Whitham 1974). As shown by KH, one of these waves represents a generalized Kelvin wave that is trapped against the coast and has a phase speed greater than the alongshore velocity of the mean flow $V(y,t)$—that is, this wave is advected by the mean intrusion (Fig. 1b), while the other is trapped against the density front and, because it has a phase speed less than $V(y,t)$, propagates upstream relative to the mean flow.

Since both waves are nonlinear, steepening of the wave front must occur. Ultimately, a shock will form at the leading edge unless the dispersive effects that result from the alongshore action of the mean intrusion are strong enough. To determine what happens when nonlinear and dispersive effects balance, KH expand the variables in (2.9) in terms of the perturbation parameter d^2 and equate the nonlinear tendency (at order d^2) with the dispersive—the case where they do not balance is considered later. Introducing a slow time scale on which the nonlinear and dispersive effects are

important and are given by the original scale $1/df$ divided by d^2, KH show that a balance exists on this scale as described by the Korteweg–deVries (KdV) equation for the wave amplitude A:

$$\frac{\partial A}{\partial T} + nA\frac{\partial A}{\partial \Omega} + p\frac{\partial^3 A}{\partial \Omega^3} = 0, \qquad (2.17)$$

where n and p are constant coefficients describing the nonlinear and dispersive terms, respectively, and A is the wave amplitude on the slow time scale T;

$$T = d^{-3}f^{-1} = \left[\frac{RH}{aL^*}\right]^{-5} f^{-1} \qquad (2.18)$$

and Ω is a phase variable that depends on the linear long-wave speed $c_0 = \sqrt{g'H}$, the alongshore displacement y, and the original time scale t as

$$\Omega = (y - c_0 t). \qquad (2.19)$$

The Appendix contains this analysis extended for the case where the coastal mountains do not act as an impermeable barrier (as assumed for the coast by KH) but are porous to some extent to simulate the effects of gaps. This analysis then leads to an inhomogeneous Korteweg–deVries–Burgers (KdVB) equation for the wave amplitude:

$$\frac{\partial A}{\partial T} + nA\frac{\partial A}{\partial \Omega} + p\frac{\partial^3 A}{\partial \Omega^3} + \sigma\frac{\partial^2 A}{\partial \Omega^2} = \mu u^*, \qquad (2.20)$$

where σ represents viscosity and μ and u^* are constants, with u^* representing the small flow that "leaks" through the mountains.

The solitary wave solution of (2.17) then leads to the familiar hump-shaped profile

$$A(\Omega) = \alpha \operatorname{sech}^2\left[\left(\frac{n\alpha}{12p}\right)^{1/2}\Omega\right], \qquad (2.21)$$

so that the marine layer depth as a whole (e.g., KH; Grimshaw 1985) is

$$h(x, y, t) = \alpha e^{+(x/R)} \operatorname{sech}^2\left[\left(\frac{n\alpha}{12p}\right)^{1/2}\Omega\right], \qquad (2.22)$$

showing the offshore exponential decay of a Kelvin wave. In (2.21) and (2.22), α is the amplitude of the solitary wave, which may be calculated from the pressure perturbation caused by the passage of this wave (Reason and Steyn 1988) and which determines the phase speed of the wave as

$$c = \sqrt{g'H(1 + \alpha)}. \qquad (2.23a)$$

A result that will be needed later is that any convex bends in the bounding wall should be less than a critical angle,

$$\phi = \sqrt{3\alpha}, \qquad (2.23b)$$

in order for the solitary wave to propagate around without separation from the wall or other loss of identity. Although (2.23b) was formally derived (Miles 1977) for a nonrotating gravity wave, it may be applied to Kelvin waves because the only effect rotation has on a Kelvin wave is to cause an exponential decay of amplitude and alongshore velocity away from the bounding wall—in all other respects, a Kelvin wave behaves like a nonrotating gravity wave (e.g., Gill 1982).

The slow time scale T describes the evolution time for the solitary wave from the initial intrusion. Note that T is sensitive to the ratio of the Rossby radius to the alongshore length scale and the nonlinear parameter a/H. Thus, waves with R/L^* not much less than unity (weakly semigeostrophic) and that are weakly nonlinear (a/H small) will evolve more quickly. Predictions of T from (2.18) will be compared with observations for the North American and Australian disturbances in sections 3b–d.

Evolution of an intrusion into nonlinear and eventually solitary waves has been observed in the atmosphere for small-scale, nonrotating flows on the nocturnal inversion layer in northern Australia (Christie et al. 1978, 1979), in rotating-tank experiments (Maxworthy 1983; KH; Simpson 1987), and in the coastal ocean (KH; Griffiths 1986; Paldor 1988). It is considered here that a similar situation may occur for the coastally trapped ridges of western North America and southeastern Australia.

It is important to realize that solitary forms of the nonlinear waves will only develop if dispersive effects are sufficiently strong to balance the nonlinear steepening. Dispersive effects occur via the action of the mean flow, largely alongshore in direction, or through the existence of an appropriate background flow. If, however, significant across-shore flow occurs near the leading edge of the intrusion, then dispersive effects are too weak to provide the balance necessary for solitary wave evolution (KH). Instead, these authors show that the semigeostrophic theory breaks down near the leading edge of the intrusion and a shock forms there. By assuming conservation of mass and momentum, KH show that the leading edge of the intrusion propagates as the shock wave form of the nonlinear Kelvin wave on an evolution time T given by (2.18) and with speed given by

$$c = 1.45\sqrt{g'H_u}, \qquad (2.24)$$

where H_u is the fluid depth upstream of the shock (i.e., upstream of the leading edge). Equation (2.24) has been confirmed in rotating-tank experiments (Griffiths and Hopfinger 1983; KH; Griffiths 1986). Note, though, that Griffiths and Hopfinger (1983) found the proportionality factor to be 1.3 rather than 1.45. The parameter H_u is not necessarily the same as H, the undisturbed fluid depth that is used in the long wave

speed formula $\sqrt{g'H}$. For example, in rotating-tank experiments, H_u is taken as the depth immediately behind the head of the intrusion (KH; Griffiths 1986).

3. Application of the theoretical model to three coastal ridging events

a. Introduction

It is once again emphasized that the mesoscale nature of the ridges presents problems in obtaining data of sufficiently high spatial and temporal resolution. Despite this sparsity of data, it is believed that enough exists to provide an adequate test of the above theory. Analysis of Figs. 2–10 will show that this theory is qualitatively, and in many instances quantitatively, consistent with available observations.

Since the Australian case of November 1982 exhibits both Kelvin wave and gravity current behavior (Holland and Leslie 1986), it would seem to be the most obvious candidate for the theory and is therefore considered first.

b. Australian event of November 1982

Following an analysis of the observed marine-layer winds, pressure and temperature fields, and displacement of the inversion, Holland and Leslie (1986) considered the coastal ridging event of 9–11 November 1982 in southeastern Australia that propagated from Mount Gambier (see Fig. 2 for place locations) on the south coast to Brisbane on the east coast, to develop initially as a coastal intrusion. Because the ridge propagated too quickly on the south coast to be just a gravity current, and because it had no difficulty in negotiating the sharp convex bend in the coastline at Gabo Island, these authors considered the ridge to evolve as a superimposed nonlinear Kelvin wave that propagated through and ahead of the main current. This hypothesis was supported by a fine-mesh primitive equation model of the coastal ridge (Holland and Leslie 1986) in which a disturbance was seen to evolve and propagate through the main body of the ridge—it is also consistent with the theory of section 2 and the rotating-tank experiments of KH, Maxworthy (1983), and Simpson (1987). Since the winds near the leading edge of the ridge are alongshore (Holland and Leslie 1986, Fig. 9; Reason 1989), it is expected (KH, section 2) that the superimposed Kelvin wave will be of solitary rather than shock form.

From Holland and Leslie's (1986) data of reduced gravity $g' = 0.6$ m s^{-2} and lower layer depth $H = 1500$ m for the south coast, one calculates a Rossby radius $R = 327$ km. The alongshore length scale L^* is taken as the product of the observed speed and time scale of propagation (20 m s^{-1} and 14 h, respectively), and hence $L^* = 1008$ km. Using the observed (Holland and Leslie 1986) pressure displacements caused by the propagation of the coastal ridge, the ratio H/a is calculated as about 2 (Table 1). Substitution into (2.18) then gives an evolution time for the Kelvin wave component of 29 h. This value is consistent with the 24 h suggested by the observed surface pressure traces (Fig. 2) and soundings and satellite imagery given in Holland and Leslie (1986).

Holland and Leslie (1986) compared the linear Kelvin wave speed (30 m s^{-1} on the south coast, 19 m s^{-1} on the east coast) with the observed (40 m s^{-1} on the south coast, 20 m s^{-1} on the east coast). Table 1 extends this comparison to include the solitary Kelvin wave speed and the empirical atmospheric gravity current speed of Seitter and Muench (1985). It is seen that only the solitary Kelvin wave speed compares favorably on the south coast, whereas on the east coast the linear Kelvin wave speed is most accurate, with the solitary wave speed reasonable. The gravity current formula is too slow on the south coast and does not have the sharp decrease on the east coast that observations and both Kelvin wave speeds show.

An important question raised by Holland and Leslie (1986) was why the ridge was able to coherently propagate around the convex bend in the coastal mountains near Gabo Island, but not around that at Brisbane. There is no theoretical explanation for this behavior for a linear Kelvin wave or for a gravity current. However, if one assumes a solitary Kelvin wave model, then application of (2.23b) can account for the observations.

Taking $\alpha = 0.57$ (0.49) observed at Mascot (Nowra) and Wilson's Promontory gives a critical angle of 75° (70°). From Fig. 2, the angle of the convex bend in the mountains (1000-m contour) at Gabo Island is seen to be about 65°, so that theoretically a solitary Kelvin wave of this amplitude should be able to propagate around without loss of identity. On the other hand, at Brisbane, $\alpha = 0.18$ so that the critical angle from (2.23b) is 42°. Figure 2 indicates that from Brisbane onwards, there are no mountains of 1000-m height until the range just south of Townsville (about 700 km to the north of Brisbane) and that the 600-m contour bends about 50°. Thus, it is expected that a solitary Kelvin wave of this amplitude will not be able to propagate farther than Brisbane but instead, will separate from the coastal mountains and lose its identity. Satellite imagery in Holland and Leslie (1986) indicates that this is precisely what happens. Further confirmation of the inability of the ridge to propagate beyond Brisbane can be seen from the barograph trace (Fig. 2) for Rockhampton, which shows no record of the pressure rises observed to the south. Thus, it is seen that the observed behavior of propagation of the ridge around the convex bend at Gabo Island but not at Brisbane is consistent with solitary Kelvin wave theory.

Although the solitary Kelvin wave model is successful in predicting the behavior of the ridge at convex bends and the propagation speed, both the shape of the pressure traces in Fig. 2 and the observed decrease

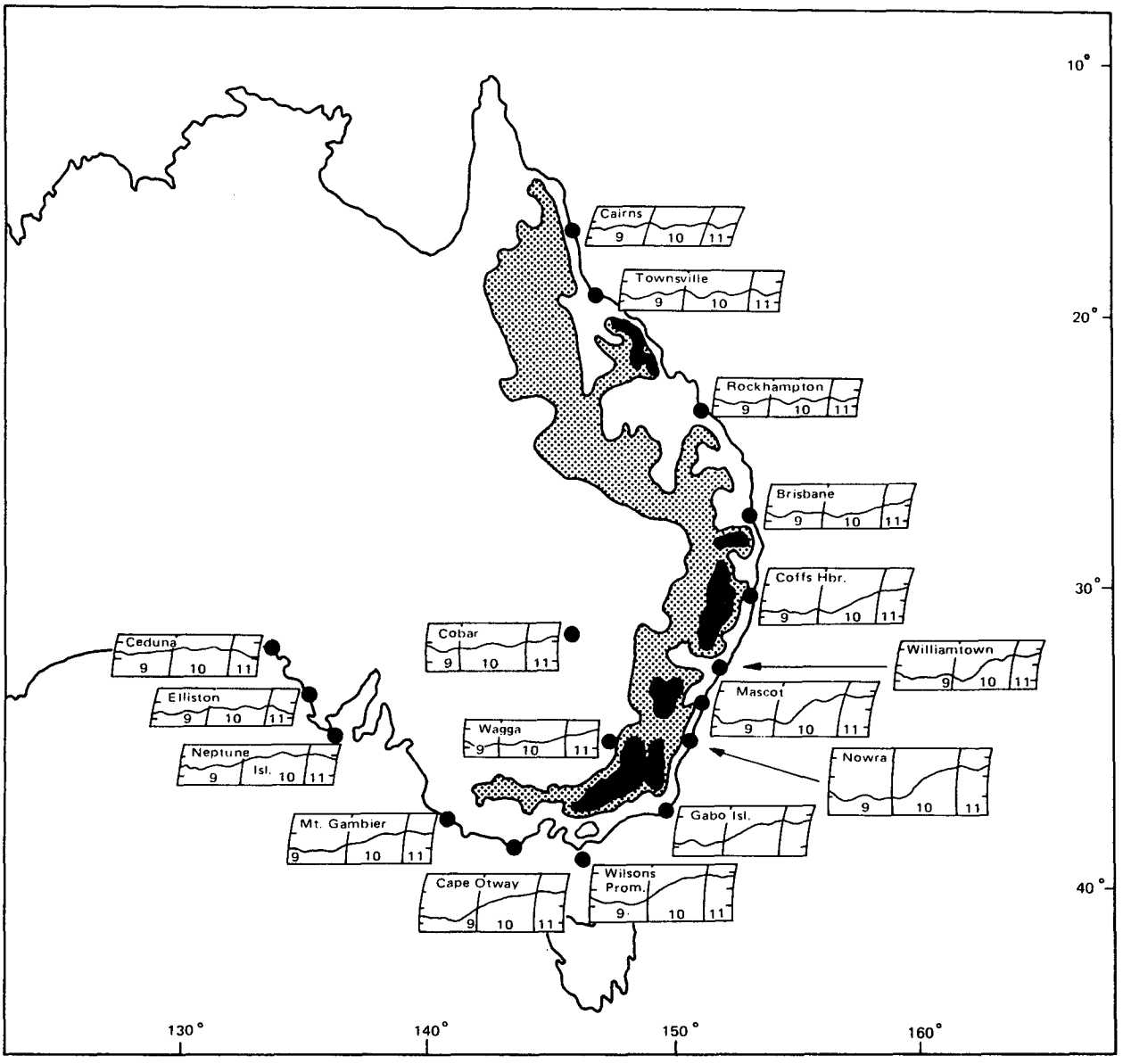

FIG. 2. Barograph traces of surface pressure for various inland and coastal stations in eastern Australia over the period 0000 UTC 9 November–1200 UTC 11 November 1982. The tick marks on each trace are at 10-mb spacing. Unshaded regions are at 0–600-m elevation, stippled regions at 600–1000-m elevation, and shaded areas refer to terrain over 1000 m in elevation. Adapted from Holland and Leslie (1986).

in amplitude and loss in sharpness of the wave front with propagation northwards indicate that a more sophisticated model may be necessary. Since the most pronounced weakening [i.e., reduced displacement of the lower layer and less pronounced wind shifts and southerly winds; see Holland and Leslie (1986)] of the coastal ridge was observed to occur in the vicinity of large valleys, the KdVB model (2.20) of section 2 with damping due to gaps or valleys in the coastal mountains may be more appropriate. In the homogeneous case, the KdVB equation describes a wave amplitude decay proportional to $1/T$, where T is the slow time scale (2.18) (Grimshaw 1983), whereas in the nonhomogeneous case, Smyth (1988) has shown that the decay is less than l/T. It is now shown that this form of decay agrees qualitatively with the observations.

The theoretical amplitude was calculated according to the $1/T$ decay from the observed value at Nowra of 0.49 to be 0.30 at Brisbane (Reason 1989), as compared with the observed value of 0.18. Despite that the KdVB model has assumed a constant dissipative loss due to gaps in the mountains all along the propagation

TABLE 1. Speeds of propagation and observed amplitudes of the Australian coastal ridge. Gravity current (GC), from Seitter and Muench (1985), $c = 0.79\sqrt{\Delta p/\rho}$, where Δp is pressure difference between gravity current head and ambient air, ρ is density of ambient air; linear Kelvin wave (LKW): $c = \sqrt{g'H}$; Solitary Kelvin wave (SKW): $c = \sqrt{g'H(1 + \alpha)}$; Observations are Mascot (M), Nowra (N), Williamtown (W), Brisbane (B), Mount Gambier, (G), Cape Otway and Wilson's Promontory (O), and Neptune Island (NI).

Coast	Observed speed (m s^{-1})			Computed speed (m s^{-1})	Scaled amplitude (−)	Pressure difference (mb)
South	40	SKW		37.6	0.57	
		LKW		30.0		
		GC	(NI)	16.0		5
			(G)	22.6		10
			(O)	30.2		18
East	20	SKW	(M)	23.8	0.57	
		SKW	(N)	23.2	0.49	
		SKW	(W)	23.4	0.52	
		SKW	(B)	20.6	0.18	
		LKW		19.0		
		GC	(N)	27.6		15
			(M)	27.6		15
			(W)	29.4		17
			(B)	22.6		10

path between Nowra and Brisbane (Fig. 2 indicates three gaps), the analysis, as it stands here, is sufficiently robust to indicate the probable importance of gaps in the mountains on the coastal ridge.

Further confirmation of the appropriateness of the KdVB model comes from a comparison of the displacement of the surface pressure (Fig. 2) and temperature fields (see Figs. 7–9 of Holland and Leslie 1986) with the displacement structure expected from the model. For long enough times, Johnson (1970, 1972), Whitham (1974), and Smyth (1988) showed that the KdVB equation has a steady, undular bore solution. Figure 3, taken from Whitham, illustrates one such steady-state solution for the case where the dissipation allows an undular decay to the asymptotic end state rather than the monotonic decrease for stronger dissipation. Unfortunately, the available data do not allow all the coefficients in the KdVB equation to be evaluated, so it is not possible to determine the strength of the dissipation relative to the nonlinear and dispersive terms in the model. Qualitatively, however, the similarity between the undular bore solution of Fig. 3 and the observations of Fig. 2 (and Figs. 7–9 in Holland and Leslie 1986) provides further evidence of the appropriateness of a KdVB model for the propagation of the coastal ridge along the east coast between Nowra and Brisbane.

c. *California event of 3–7 May 1982*

On the basis of the observed displacement of the marine-layer wind and pressure fields and the inversion height and a comparison of the observed width and speed of the ridge with theory, Dorman (1985, 1988) considered the May 1982 coastal ridge that propagated from Point Conception to Cape Mendocino (see Fig. 4) to be a solitary Kelvin wave propagating in the marine layer. This conclusion was disputed by Mass and Albright (1987, 1988), who considered that the event was a response to the interaction of synoptic pressure changes with the topography in which the coastal winds consisted of two components. One component, the ageostrophic one, was controlled by the synoptic-scale alongshore pressure distribution, while the other, the geostrophic one, was determined by the pressure gradient normal to the coast (Mass and Albright 1987). It must be emphasized that the objective here is not to determine which author is correct, but rather to point out that when synoptic-scale pressure changes are included in the dynamics, both the Dorman and the Mass and Albright hypotheses appear as components of a more general interpretation of this event.

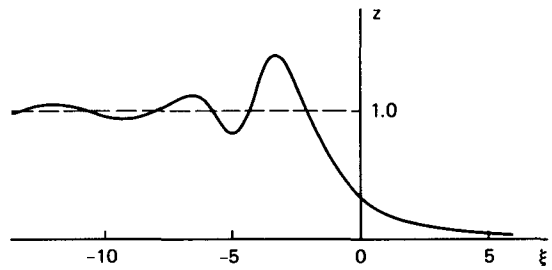

FIG. 3. Steady-state, undular bore solution of the Korteweg–deVries–Burgers equation. The normalized variables z and ξ are proportional to interface displacement and wave front propagation distance, respectively. Adapted from Whitham (1974).

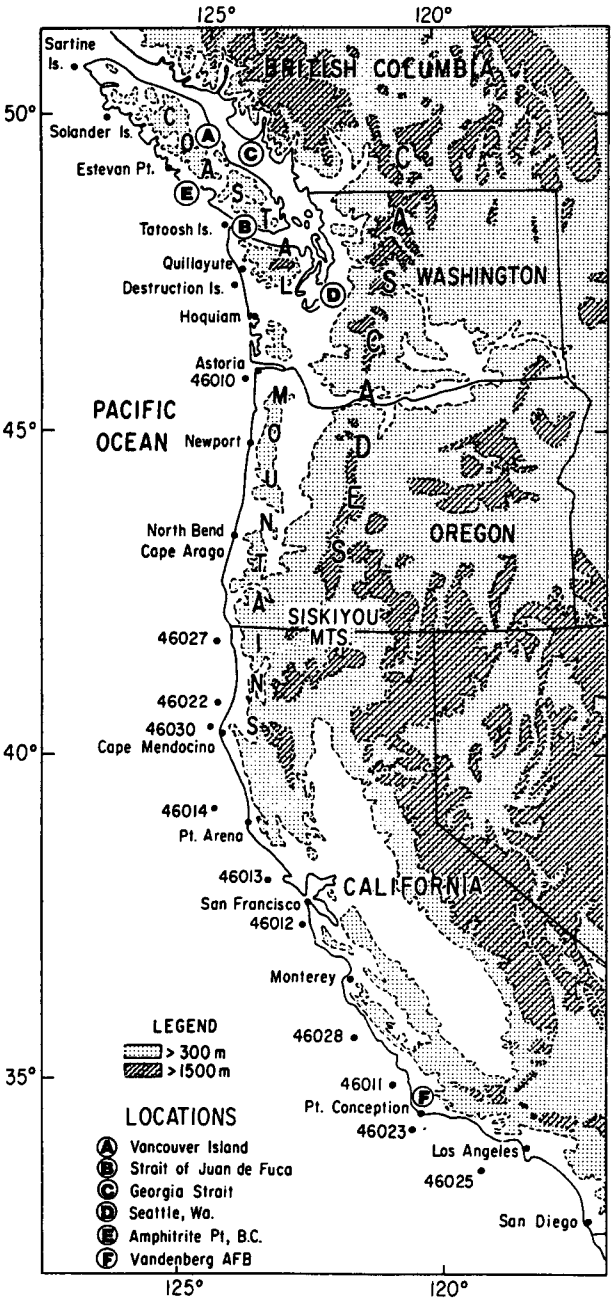

FIG. 4. Topographic and place location map of the west coast of the United States and southern British Columbia, Canada. Adapted from Mass and Albright (1987).

Consideration of (2.4)–(2.5) shows that when a synoptic pressure gradient $(\partial P/\partial x, \partial P/\partial y)$ is included in the equations, the Mass and Albright hypothesis does not contradict a forced model consisting of a coastal intrusion with an associated nonlinear Kelvin wave—in fact, the analysis of section 2 based on these equations explicitly contains these two components where our semigeostrophic part is exactly what Mass and Albright (1987) term as their geostrophic component. The forced nonlinear Kelvin wave model of Gill (1977), in which u is identically zero everywhere, contains a more specialized version of these two components. Thus, (2.12) gives the coastal wind component that is in geostrophic balance with the pressure gradient normal to the coastal mountains, while the solution to (2.16) contains the ageostrophic downgradient component. The analysis of the latter part of section 2 showed that this component has a solitary Kelvin wave part associated with it that develops on the time scale given by (2.18). It is clear, therefore, that in this more general treatment of the dynamics, both the Dorman and the Mass and Albright hypotheses are present. Thus, this objection of Mass and Albright (1987) does not negate the existence of a nonlinear Kelvin wave in the dynamics when synoptic forcing is included. However, their objection is valid for a free Kelvin wave model and a quote from Mass and Albright (1988) reveals that such a model may be what they had in mind: "the question is whether this change was freely propagating or controlled by synoptic-scale changes. We believe the evidence shows the latter to be the case."

It is now argued that other objections made by Mass and Albright (1987, 1988) to the existence of a Kelvin wave, while valid for the linear free case, do not negate a nonlinear, synoptically forced wave. The point of Mass and Albright that pressure changes were observed inland from the coastal mountains may be countered by two observations. First, the significant gap in the coastal mountains at San Francisco allows marine-layer changes to be communicated to the interior and, as Bannon (1981) has shown, the synoptic forcing may generate a disturbance inland of the coastal mountains in addition to the coastal one. Second, it is likely that much of the observed interior pressure changes directly result from the midlevel westerly passage of the synoptic low that also forced the coastal event. Another point made by Mass and Albright was that the observed wind shift and pressure changes did not appear in phase. As shown by Gill (1977), nonlinear effects result in a lag between the changes in coastal wind and pressure fields and inversion height associated with the passage of a nonlinear Kelvin wave, and so one should not always expect to observe simple wave displacements in the data. In summary, it is felt that neither the Dorman nor Mass and Albright hypotheses are excluded but that the theory of section 2 offers a more constructive explanation. That is, the synoptic pressure changes force an ageostrophic downgradient flow that is topographically trapped and that has a solitary Kelvin wave associated with it.

Whether or not a solitary Kelvin wave component develops depends (KH and section 2) on whether there are significant across-shore winds near the leading edge of the initial flow. Since the winds here were predominantly alongshore [Figs. 2, 8, and 14 of Dorman (1985) and Figs. 26 and 29 of Mass and Albright

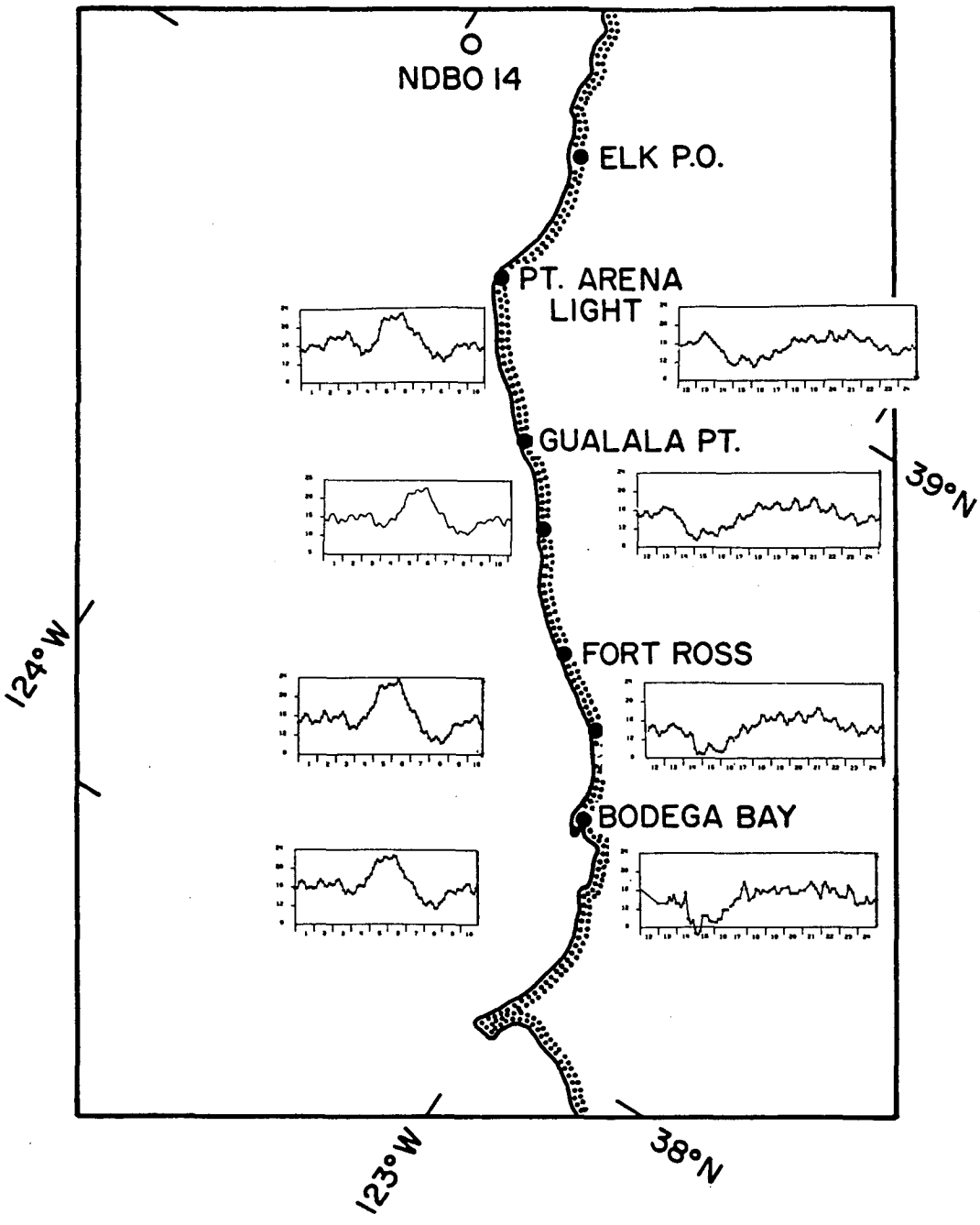

FIG. 5. Surface pressure traces for various stations along the central Californian coast for the May 1982 (left-hand plot in each case) and July 1982 (right-hand plot in each case) events. On the vertical axis of each trace, the numbers (xx) refer to $10xx$ millibars, while the horizontal axis gives the day in either May or July.

(1987)], a solitary Kelvin wave rather than a shock Kelvin wave is expected to develop. On the other hand, the July (1982) event analyzed by Dorman (1987) and section 3d did show significant across-shore winds, and therefore a shock Kelvin wave rather than a solitary one is expected (KH and section 2).

Figure 5 compares a series of surface pressure traces for the May 1982 event with those of the July 1982 gravity-current event studied by Dorman (1987). The pressure traces are taken along the central California coast between 38° and 39°N and were obtained during the CODE field program (see Fig. 4 for the relation of the stations to the coastal mountains). Unfortunately, the program did not extend over the entire propagation

path of the ridges from Point Conception (35°N) to Cape Mendocino (40°N–May 1982) or Cape Blanco (42°N–July 1982). It is clear from Fig. 5 that the May 1982 event resulted in a pulselike, hump-shaped displacement of the surface pressure consistent with a solitary Kelvin wave, whereas the July 1982 event showed long-term, irregular, and variable displacement as expected for a gravity current with a shock at the leading edge (Dorman 1987; Simpson 1987). Similar behavior was observed in the inversion height data by Dorman (1985), who also found a steady alongshore progression of wind changes (his Fig. 8) and stratus cloud cover throughout the event.

Also consistent with the existence of a solitary Kelvin wave component is that the observed surface pressure and wind data (Figs. 5, 6) vary gradually during the event and do not show the abrupt (i.e., occurring in minutes) changes typical (Simpson 1987) of gravity currents with a leading shock.

Further support for the existence of a solitary Kelvin wave component comes from a comparison of the theoretical propagation speed with the observed speed (6 m s^{-1}; Dorman 1985) of the ridge. Mass and Albright (1987) made no attempt to account for this observed speed, whereas Dorman (1985) computed the linear Kelvin wave speed (3.7–6.0 m s^{-1}). Using (2.23a), where the amplitude α was calculated as 0.161 by Reason and Steyn (1988) from Dorman's (1985) data, the net solitary Kelvin wave speed may be computed as 4.0–6.5 m s^{-1} after the mean opposing wind

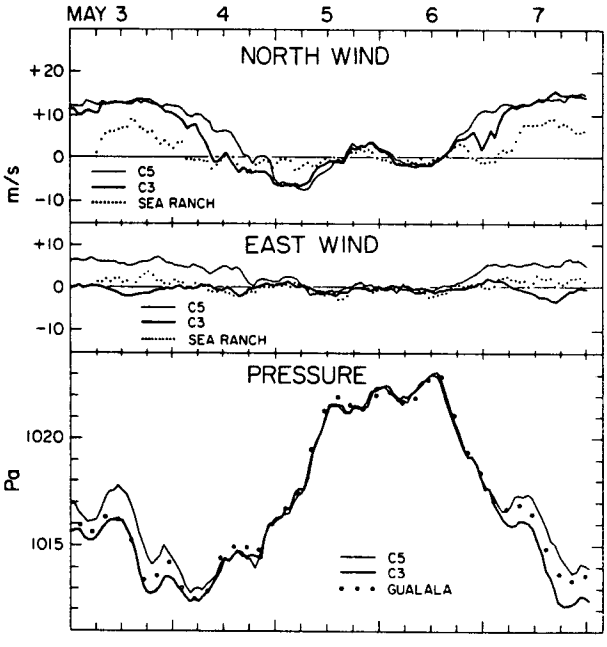

FIG. 6. Surface winds and pressures for Gualala station and offshore buoys on the central Californian coast during the May 1982 event. The winds have been rotated so that "North" is actually 317°, aligned with the coast. Station Sea Ranch is located on the coast a few kilometers south of Gualala. Adapted from Dorman (1985).

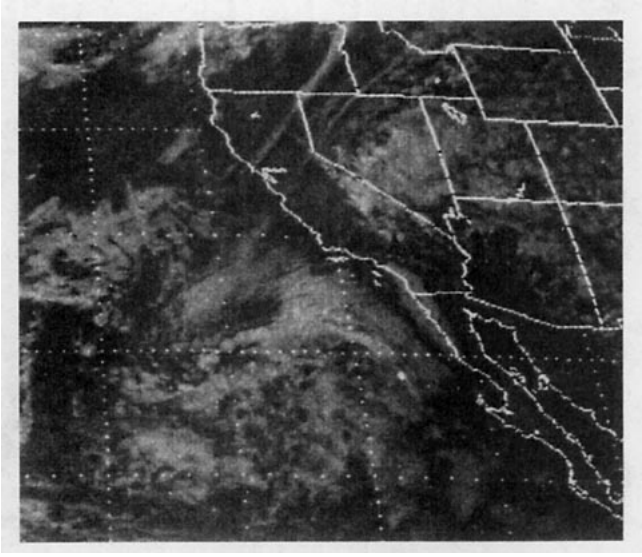

FIG. 7. GOES-West satellite visible imagery for 0045 UTC 3 May 1982. The localized initial displacement (low-level stratus deck) of the marine layer in the Southern Californian Bight is evident. Note the trapping by the coastal mountains. (Courtesy of C. Dorman.)

observed by Dorman (1985) has been subtracted. On the other hand, using the empirical formula for an atmospheric gravity current (Seitter and Muench 1985; defined in Table 1) gave a speed of less than 3 m s^{-1}. It is clear that only the Kelvin wave formula agrees reasonably well with the data, with the solitary version giving better agreement than the linear one.

Finally, the observed cessation of the propagating coastal ridge at Cape Mendocino was explained theoretically by Reason and Steyn (1988) using equation (2.23b) valid for a solitary Kelvin wave. On the other hand, Mass and Albright (1987) were unable to provide a convincing explanation for the cessation of the event.

The parameters needed by (2.18) to determine the evolution time scale of this event are as follows. From Dorman (1985), the computed Rossby radius R for a Kelvin wave was obtained from sounding data for the central Californian coast as 150 km. This value was seen to agree favorably with the observed width of the coastal ridge there (Dorman 1985). The amplitude ratio a/H was calculated by Reason and Steyn (1988) from Dorman's data as 0.161. To determine the alongshore length scale L^* required in (2.18), the observed (Dorman 1985) propagation speed for the disturbance of 6 m s^{-1} is multiplied by the time span between the leading and trailing edges of 3.1 days (see Fig. 13 of Dorman 1985) to give an estimate for L^* of 1600 km.

Substituting the above parameters into (2.18) then gives an evolution time T for the solitary Kelvin wave of 46 h. Such a value for T is consistent with the observations of the inversion displacement (Fig. 15 of Dorman 1985), which show the inversion to reach a maximum height 36 h after the initial raising of the marine layer. Also, satellite images (Figs. 7, 8, and 9)

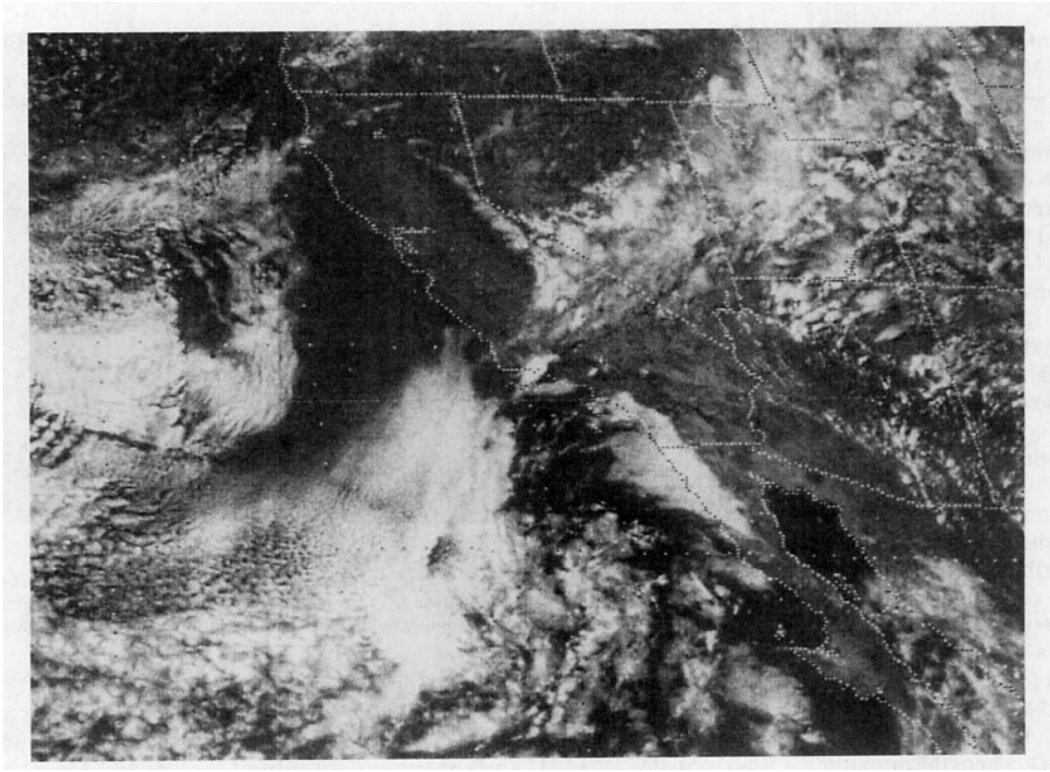

FIG. 8. GOES-West satellite visible imagery for 2315 UTC 3 May 1982. Some erosion of the stratus cloud due to diurnal heating is evident on comparison of the stratus deck with that shown in Fig. 1. Note that UTC is 7 h ahead of local time. (Courtesy of C. Dorman.)

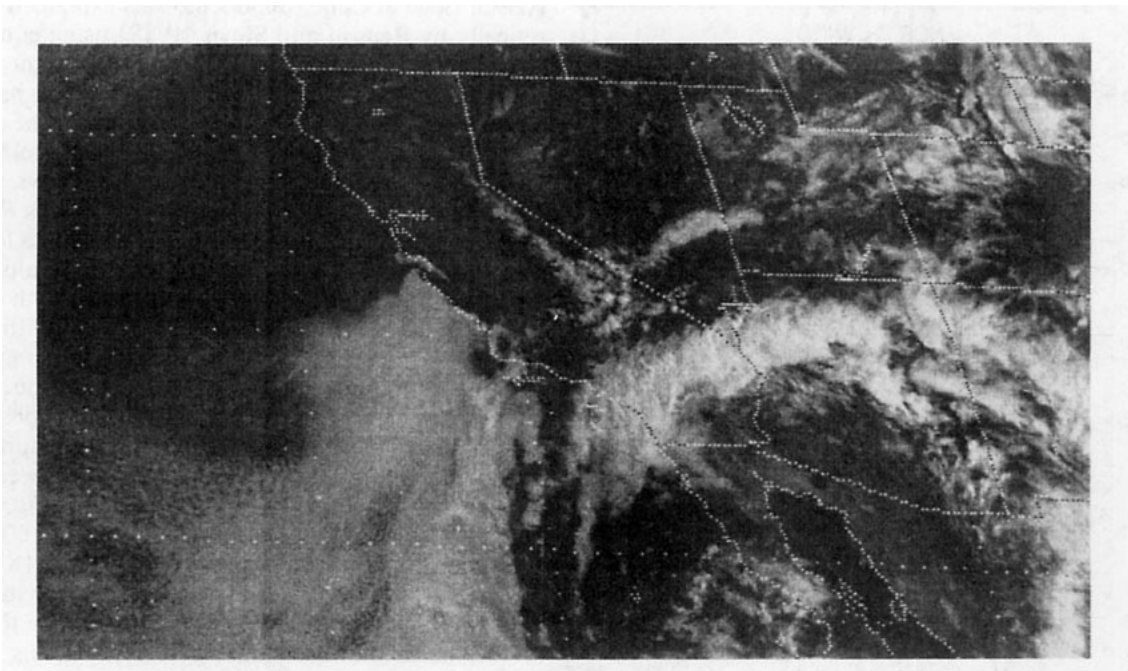

FIG. 9. GOES-West satellite imagery for 1515 UTC 4 May 1982 showing the propagation of the stratus deck to Monterey Bay south of San Francisco. (Courtesy of C. Dorman.)

of the Californian Bight region where the disturbance was generated show the initial marine-layer disturbance (generated around 0045 UTC May 3) still within the bight at 1515 UTC May 3, but by 1515 UTC the next day, the disturbance had already propagated 100 km or so northwards along the coast. Thus, from these images, the evolution time of the solitary Kelvin wave would be 23–38 h. The theoretical scale of 46 h is therefore seen to be consistent with the available observations.

In summary, it is clear that a model forced by synoptic-scale pressure changes and whose response includes a solitary Kelvin wave component can explain all the salient features of the May 1982 event. The arguments given by Mass and Albright (1987) for negating the existence of a Kelvin wave have been shown above to be invalid for a synoptically forced solitary Kelvin wave, although they do hold true for the free linear case.

d. California to Oregon event of 13–20 July 1982

As shown in Dorman (1987), the coastal ridging event that propagated from Point Conception (35°N) to southern Oregon during July 1982 was characteristic of a coastally trapped gravity current with a steep leading edge. Since significant across-shore winds were initially observed (Figs. 3, 7, and 12 of Dorman 1987) near the leading edge of this coastal ridge, it is expected (section 2; KH) that by time T (2.18) a shock wave evolves at the leading edge with propagating speed given by (2.24). From Dorman (1987), the disturbance along the central and northern California coasts was observed to travel at 8.8 m s^{-1}. Application of (2.24) requires g', which is 0.3 m s^{-2} from Dorman, and the upstream marine-layer depth H_u, which can be estimated from the Vandenburg (see Fig. 4 for place locations) sounding data (Fig. 10) as 450 m. This value is chosen because, according to KH, H_u must be taken as the fluid depth immediately behind the head of the intruding gravity current or equivalently as that observed after this leading head has passed; hence, for Vandenburg, the value of 450 m observed on 18 July after the maximum inversion displacement associated with the gravity-current head is appropriate. Thus, the computed shock-wave speed is 16.8 m s^{-1} [or 15.1 m s^{-1} if the constant = 1.3 as in the experiments of Griffiths and Hopfinger (1983)]. Opposing this is a mean northerly wind of 7.5 m s^{-1} (Fig. 8 of Dorman 1987), which then gives a net propagation speed of 9.3 m s^{-1} (or 7.6 m s^{-1}) as compared with the observed 8.8 m s^{-1}. Dorman, however, used the linear Kelvin wave speed that gave 12.0 m s^{-1} along this coast and, hence, a net propagation speed of 4.5 m s^{-1}, considerably less than the observed speed. Applying the empirical (Seitter and Muench 1985) gravity-current formula (defined in Table 1) gives 5.0 m s^{-1}. Hence, the shock Kelvin wave speed of (2.24) agrees most favorably with the data.

The shock wave formulation of KH is also able to explain, to some extent, another discrepancy noted by Dorman (1987), namely that between the observed

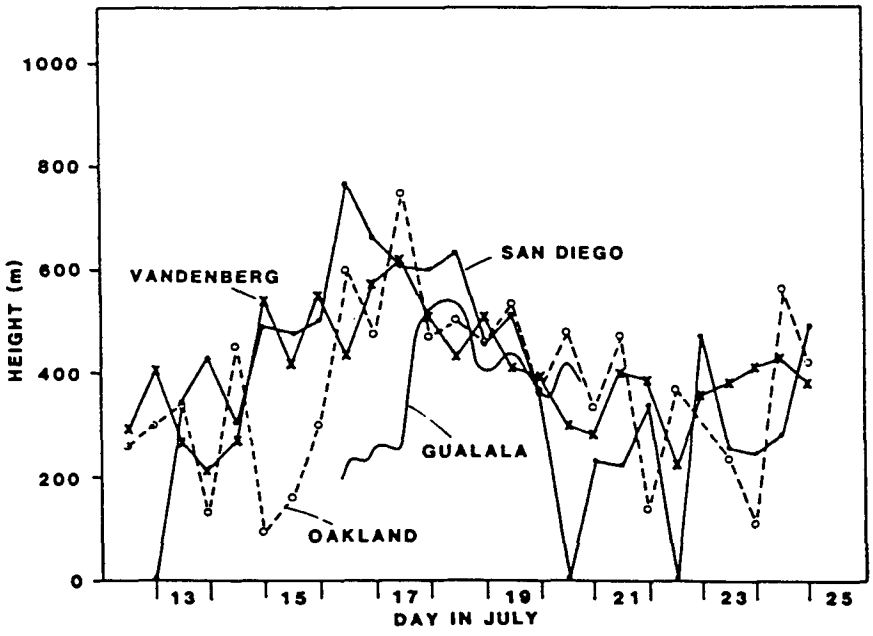

FIG. 10. Height of the base of the inversion at San Diego, Vandenburg, Oakland, and Gualala during the July 1982 event. Adapted from Dorman (1987).

width of the disturbance and the Rossby radius. Although agreement is satisfactory (within 10%) south of 36°N, along the central and northern Californian coasts (e.g., at Point Arena, 38°N) and in southern Oregon (43°N), discrepancies arise. From Dorman (1987), the observed width at 38°N is 60 km and the Rossby radius is 136 km, whereas at 43°N these parameters are 40 km and 123 km, respectively. However, using the shock wave formulation, the Rossby radius is computed on the basis of H_u and the theoretical width of the disturbance in this case is then less than or equal to 0.7 times this Rossby radius (KH; Griffiths 1986). Rotating-tank experiments (Griffiths and Hopfinger 1983) yielded the constant as 0.6 rather than 0.7. Using $H_u = 450$ m as before then gives theoretical widths at 38°N and 43°N of less than 90 km and 81 km (or 77 km and 69 km if the empirical 0.6 constant is used), respectively.

Application of (2.18) to determine the evolution time of the shock wave is now considered. From Dorman (1987), $R = 143$ km on the central Californian coast. The alongshore length scale L^* is estimated as 1521 km from the product of the observed propagation speed (8.8 m s^{-1}) and the time scale of propagation (2 days). The parameter a is estimated as the difference between the climatological value of the inversion along the central Californian coast (400 m; Beardsley et al. 1987) and the mean value observed during the event (480 m; Dorman 1987). Hence, $H/a = 480/80$, and after substituting in (2.18), a theoretical evolution time for a shock coastal wave of 54 h is obtained. Since the disturbance was observed to take 2 days to begin propagating after the initial raising of the marine layer in the California Bight (Dorman 1987), it is clear that the theoretical evolution time is reasonable.

4. Discussion

The dynamics of coastally trapped ridges in the lower atmosphere have been treated with a nonlinear semigeostrophic theory. This treatment of the dynamics provides a more general theoretical framework than hitherto available and generalizes beyond the specific interpretations of Dorman (1985, 1987, 1988), Holland and Leslie (1986), and Mass and Albright (1987, 1988). Thus, there is an alongshore ageostrophic downgradient flow influenced by synoptic-scale pressure changes as envisaged by Mass and Albright (1987, 1988), but associated with this intruding flow, either a solitary Kelvin wave or a shock Kelvin wave may develop depending on the winds near the leading edge of the intrusion. Significant across-shore winds (July 1982 California case) lead to shock development, whereas alongshore winds (May 1982 California and November 1982 Australian cases) allow a solitary Kelvin wave. The nonlinear effects that result in the solitary Kelvin wave or shock develop on a slow time scale that depends on the fundamental scales of the coastal ridge (Rossby radius, alongshore length scale, amplitude of inversion displacement).

Application of the theory gave evolution time scales and propagation speeds that agreed reasonably with the observations of Dorman (1985, 1987) and Holland and Leslie (1986). The theory was also able to explain the observed behavior of the coastal ridges at sharp convex bends in the coastal mountains at Cape Mendocino (May 1982 California event) and at Gabo Island and Brisbane (Australia event). Modification of the solitary Kelvin wave model to include the dissipative effects of gaps in the coastal mountains, so that the governing KdV equation becomes a KdVB equation, was successful in explaining the observed amplitude decay of the Australian coastal ridge.

Coastally trapped disturbances in the lower atmosphere are also common in southern Africa, but they are generally mesoscale lows rather than ridges (Gill 1977; Anh and Gill 1981; Bannon 1981; Reason and Jury 1990). This difference is due to synoptic forcing producing offshore rather than onshore flow during their generation (Reason and Jury 1990; Reason and Steyn 1990).

It appears that the nonlinear semigeostrophic theory developed in this paper has clarified to some extent the uncertainties and unresolved questions in the previous studies by Dorman (1985, 1987, 1988), Holland and Leslie (1986), and Mass and Albright (1987, 1988). There are, however, many details of the dynamics of the coastally trapped ridges that need to be better understood. These details concern the structure of the leading edge of the ridges, the exact way in which they are generated, and the possible contribution of thermal and frictional contrasts between land and ocean.

Acknowledgments. CJCR gratefully acknowledges graduate student funding in the form of a University of British Columbia Graduate Fellowship, a teaching assistantship, and a partial NSERC research assistantship. The research was supported by grants from the Atmospheric Environment Service of Environment Canada and NSERC. We are grateful to Dr. C. Dorman for helpful discussions and for providing us with the satellite images.

APPENDIX

KH Analysis Extended to a Porous Barrier

The purpose of this section is to outline the KH method and to extend it to the case where dissipation of the energy of coastally trapped disturbances due to gaps in the coastal mountains occurs.

From (2.9)–(2.14a) and following KH, consider solutions consisting of a semigeostrophic component and a small ageostrophic component, that is, let

$$v = v_{S0}(x) + \epsilon\{v_{S1}(x, y, t) + d^2 v_a(x, y, t)\} \quad \text{(A1)}$$

$$h = h_{S0}(x) + \epsilon\{h_{S1}(x, y, t) + d^2 h_a(x, y, t)\} \quad (A2)$$

$$u = \epsilon\{u_{S1}(x, y, t) + d^2 u_a(x, y, t)\}, \quad (A3)$$

where v_{S0} and h_{S0} are the components of the vector $\mathbf{V}_0$, v_{S1} and h_{S1} are components of the vector $\mathbf{V}_1$, v_a and h_a are the components of the vector $\mathbf{V}_2$, and $\epsilon \ll 1$. The vectors $\mathbf{V}_0$, $\mathbf{V}_1$, and $\mathbf{V}_2$ are related to $\mathbf{V}$, defined in the characteristic equation (2.14a) by

$$\mathbf{V} = \mathbf{V}_0 + \epsilon\mathbf{V}_1 + \epsilon^2\mathbf{V}_2 + \cdots.$$

Setting $d^2 = O(\epsilon)$, (2.4)–(2.6) become

$$(v_{S1})_t + v_{S0}(v_{S1})_y + [(v_{S0})_x + 1]u_{S1} + (h_{S1})_y + \epsilon\{v_{S1}(v_{S1})_y + u_{S1}(v_{S1})_x + \theta[(v_a)_t + v_{S0}(v_a)_y + ((v_{S0})_x + 1)u_a + (h_a)_y]\} = O(\epsilon^2) \quad (A4)$$

$$(u_{S1})_t + v_{S0}(u_{S1})_y + v_a + (h_a)_x = O(\epsilon) \quad (A5)$$

$$(u_{S1})_y - (v_a)_x + k^2 h_a = O(\epsilon), \quad (A6)$$

where $\theta = d^2/\epsilon$. Note that the forcing synoptic pressure gradient has been neglected here for simplicity. From the method of characteristics, $\partial_t = -c_\pm \partial_y + O(\epsilon)$, where $c_\pm$ are the eigenvalues of the matrix $\mathbf{B}$ in Eq. (2.14a). Substituting in (A5) and (A6) gives

$$v_a + (h_a)_x = \{c_\pm - v_{S0}(x)\} V_\pm(x)\Gamma_{\pm yy} + O(\epsilon) \quad (A7)$$

$$(v_a)_x - k^2 h_a = V_\pm(x)\Gamma_{\pm yy} + O(\epsilon), \quad (A8)$$

where

$$V_\pm(x) = \{(v_{S0}(x) - c_\pm)\mathbf{R}_\pm \cdot \nabla_{V0} v_{S0} + \mathbf{R}_\pm \cdot \nabla_{V0} h_{S0}\} / \{k^2 h_{S0}(x) + \epsilon u_y; \quad (A9)$$

$\nabla_{V0} = [(\partial/\partial V_0)], (\partial/\partial L_0)$, and V_0, L_0 are the components of the vector $\mathbf{V}$ defined in (2.14a). Here $\mathbf{R}_\pm$ is the right eigenvector of matrix $\mathbf{B}$.

$$\mathbf{V}_1 = \mathbf{R}_\pm\Gamma_\pm + O(\epsilon)$$

Following KH, v_a and h_a can be written as

$$v_a = f_\pm(x)\Gamma_{\pm yy} + O(\epsilon) \quad (A10)$$

$$h_a = g_\pm(x)\Gamma_{\pm yy} + O(\epsilon). \quad (A11)$$

From (A6) and (A8) and the conservation of potential vorticity, (2.8),

$$u_{S1y} = V_\pm(x)\Gamma_{yy} \quad (A12)$$

$$u((v_{S0})_x + 1) = (k^2 h_{S0} + \epsilon u_y)u. \quad (A13)$$

At $x = 0$, the across-shore velocity is no longer assumed to vanish, as it does in the case of a solid wall (after KH), but is taken as $u(0) = u^*$, where $u^* \ll u$ to account for the small porous effect of gaps in the coastal mountains.

Substituting the solutions for $\mathbf{V}_1$, v_{S1}, and h_{S1} obtained by KH using standard reductive perturbation techniques, namely,

$$V_1 = \mathbf{R}_\pm\Gamma_\pm + 0.5\epsilon(\mathbf{R}_\pm \cdot \nabla_{V0})\mathbf{R}_\pm\Gamma_\pm^2 + O(\epsilon^2)$$

$$v_{S1} = \mathbf{V}_1 \cdot \nabla_{V0} v_{S0} + 0.5\epsilon(\mathbf{V}_1 \cdot \nabla_{V0})^2 v_{S0} + O(\epsilon^2)$$

$$h_{S1} = \mathbf{V}_1 \cdot \nabla_{V0} h_{S0} + 0.5\epsilon(\mathbf{V}_1 \cdot \nabla_{V0})^2 h_{S0} + O(\epsilon^2),$$

and (A9)–(A13) into (A4) and using a coordinate system moving with the linear long wave speed $c_\pm$ then gives at $x = 0$,

$$\Gamma_T + \alpha_\pm\Gamma_\pm\Gamma_{\pm\Omega} + \theta\beta_\pm\Gamma_{\pm\Omega\Omega\Omega} + \alpha_\pm\beta_\pm\epsilon\mu^{-1}u^*\Gamma_{\Omega\Omega} = \mu u^*, \quad (A14)$$

where

$\alpha_\pm = \mathbf{R}_\pm \cdot \nabla_{V0} c_\pm \cdot V_0$
$\mu = 1 - \cosh(kL_0) + kV_0 \sinh(kL_0)$
$\beta_\pm$ = const given by equation (4.9) of KH.
$\Omega = y - c_\pm t$
T is given by (2.18)

Equation (A14) is an inhomogeneous Korteweg–deVries–Burgers (KdVB) equation, which is seen to be satisfied by the nonlinear Kelvin wave at the coastal mountains ($x = 0$). When $u^* = 0$ (no gaps in the bounding wall), (A14) reduces to the KDV equation derived by KH.

REFERENCES

Anh, N. N., and A. E. Gill, 1981: Generation of coastal lows by synoptic-scale waves. *Quart. J. Roy. Meteor. Soc.*, **107**, 521–530.

Bannon, P. R., 1981: Synoptic-scale forcing of coastal lows: Forced double Kelvin waves in the atmosphere. *Quart. J. Roy. Meteor. Soc.*, **107**, 313–327.

Beardsley, R. C., C. E. Dorman, C. A. Friehe, L. K. Rosenfeld, and C. D. Winant, 1987: Local atmospheric forcing during the Coastal Ocean Dynamics Experiment. 1. A description of the marine boundary layer and atmospheric conditions over a Northern California upwelling region. *J. Geophys. Res.*, **92**, 1467–1488.

Christie, D. R., K. J. Muirhead, and A. L. Hales, 1978: On solitary waves in the atmosphere. *J. Atmos. Sci.*, **35**, 805–825.

——, ——, and ——, 1979: Intrusive density flows in the lower troposphere: A source of atmospheric solitons. *J. Geophys. Res.*, **84**, 4959–4970.

Dorman, C. E., 1985: Evidence of Kelvin waves in California's marine layer and related eddy generation. *Mon. Wea. Rev.*, **113**, 827–839.

——, 1987: Possible role of gravity currents in Northern California's coastal summer wind reversals. *J. Geophys. Res.*, **92**, 1467–1488.

——, 1988: Comments on "Coastal southerlies and alongshore surges of the west coast of North America: Evidence of mesoscale topographically trapped response to synoptic forcing." *Mon. Wea. Rev.*, **116**, 2401–2406.

Gill, A. E., 1977: Coastally trapped waves in the atmosphere. *Quart. J. Roy. Meteor. Soc.*, **103**, 431–440.

——, 1982: *Atmosphere–Ocean Dynamics*. Academic Press, 662 pp.

Griffiths, R. W., 1986: Gravity currents in rotating systems. *Ann. Rev. Fluid Mech.*, **18**, 59–89.

——, and E. J. Hopfinger, 1983: Gravity currents moving along a lateral boundary in a rotating fluid. *J. Fluid Mech.*, **134**, 357–399.

Grimshaw, R., 1983: Solitary waves in slowly varying environments. *Nonlinear Waves,* L. Debnath, Ed., Cambridge University Press, 44–68.

Holland, G. J., and L. M. Leslie, 1986: Ducted coastal ridging over southeast Australia. *Quart. J. Roy. Meteor. Soc.,* **112,** 731–748.

Johnson, R. S., 1970: A nonlinear equation incorporating damping and dispersion. *J. Fluid. Mech.,* **42,** 49–60.

——, 1972: Shallow water waves on a viscous fluid—the undular bore. *Phys. Fluids.,* **15,** 1693–1699.

Kubokawa, A., and K. Hanawa, 1984: A theory of semigeostrophic gravity waves and its application to the intrusion of a density current along a coast. Part 1: Semigeostrophic gravity waves. Part 2: Intrusion of a density current along a coast in a rotating fluid. *J. Oceanogr. Soc. Japan.,* **40,** 247–270.

Mass, C. F., and M. D. Allbright, 1987: Coastal southerlies and alongshore surges of the west coast of North America: Evidence of mesoscale topographically trapped response to synoptic forcing. *Mon. Wea. Rev.,* **115,** 1707–1738.

——, and ——, 1988: Reply. *Mon. Wea. Rev.,* **116,** 2407–2410.

Maxworthy, T., 1983: Experiments on solitary internal Kelvin waves. *J. Fluid Mech.,* **129,** 365–383.

Miles, J. W., 1977: Diffraction of solitary waves. *Z. Angew. Math. Phys.,* **28,** 889–902.

Paldor, N. A., 1988: Amplitude-wavelength relations of nonlinear frontal waves on coastal currents. *J. Phys. Oceanogr.,* **18,** 753–760.

Reason, C. J. C., 1989: Coastally trapped disturbances in the lower atmosphere. Ph.D. thesis, Atmospheric Science Programme, University of British Columbia, Vancouver, 214 pp.

——, and D. G. Steyn, 1988: Comment on "Diffraction of solitary Kelvin waves at Cape Mendocino." *Mon. Wea. Rev.,* **116,** 804–805.

——, and M. R. Jury, 1990: On the generation and propagation of the Southern African coastal low. *Quart. J. Roy. Meteor. Soc.,* **116,** 1133–1151.

——, and D. G. Steyn, 1990: Coastally trapped disturbances in the lower atmosphere: Dynamic commonalities and geographic diversity. *Prog. in Phys. Geogr.,* **14**(2), 178–198.

Seitter, K. L., and H. S. Muench, 1985: Observations of a cold front with rope cloud. *Mon. Wea. Rev.,* **113,** 840–848.

Simpson, J. E., 1987: *Gravity Currents in the Environment and the Laboratory.* Ellis Horwood, 244 pp.

Smyth, N. F., 1988: Dissipation effects on the resonant flow of a stratified fluid over topography. *J. Fluid Mech.,* **192,** 287–312.

Stern, M. E., J. A. Whitehead, and B.-L. Hua, 1982: The intrusion of a density current along a coast of a rotating fluid. *J. Fluid Mech.,* **123,** 237–265.

Wadhams, P., A. E. Gill, and P. F. Linden, 1979: Transects by submarine of the East Greenland polar front. *Deep-Sea Res.,* **26A,** 1311–1327.

Whitham, G. B., 1974: *Linear and Nonlinear Waves.* Wiley-Interscience, 636 pp.

Yamagata, T., 1980: A theory for propagation of an oceanic warm front with application to Sagami Bay. *Tellus,* **32,** 73–76.